Challenging Glass 5
Conference on Architectural and Structural Applications of Glass
Bos, Louter, Belis (Eds.), Ghent University, June 2016.

Evaluation of Artificial Ageing Methods for Glass

Kyriaki Corinna Datsiou, Mauro Overend
Glass and Façade Technology Research Group, University of Cambridge, UK

Surface damage that accumulates on the surface of glass is known to govern the strength of this material. It would therefore be very useful to use artificial ageing techniques to replicate this level of damage; this would allow a rapid and cost effective assessment of the expected glass strength and the long term performance of novel glass products and treatments. Some artificial ageing methods exist but it is unclear whether the surface damage induced is correlated with the physical damage found in naturally aged glass. The aim of this paper is therefore, to evaluate available artificial ageing methods of glass using as a reference naturally aged annealed glass.

The artificial ageing methods of the as-received specimens involved the induction of: (a) a single flaw on the as-received specimens with a custom-made scratching device (SC series); and (b) uniform damage to the specimens with the use of dropped grit (SA series). Each ageing method was then evaluated with destructive and non-destructive testing. These results were then compared to those obtained from the naturally aged glass (NA series). A 65% reduction in mean strength with the respect to the as-received annealed glass was noted for the naturally aged series. This reduction was approximated (62-79%) by the artificial aged series. However, a perfect match has yet to be found especially when other fractile values of strength as well as surface roughness data are also taken into account. Nevertheless, in general the SA series were found to perform better than the SC series.

Keywords: artificial ageing, scratching device, sand trickling method, naturally aged glass

1. Introduction

The rapid technological developments in the glass industry are leading to an increasing supply of novel products in the architectural glass market. Regardless of the glass product, damage accumulates on the surface of glass during its service life and results in the formation of "Griffith flaws" that act as stress concentration points and consequently lead in strength reduction. There is currently a high degree of uncertainty when predicting the long term mechanical performance of novel glass products (e.g. treatments and coatings) partly because an artificial ageing method that is correlated with real-world damage accumulation has yet to be established.

Two are the main types of mechanical abrasion that accumulate on the glass surface during its service life: (a) damage caused by flying projectiles when the glass is part of the outer skin of the building; and / or (b) damage caused by mishandling of the glass elements during installation, cleaning and other activities during the service-life of the building.

On impact from a flying projectile, the glass either fractures or surface damage manifests itself as glass erosion i.e. material removal from the surface of the glass leading to reduction in mechanical strength and degradation of its optical quality. The erosive mechanisms on glass surfaces were investigated thus far with sand abrasion involving two approaches: (a) the sand trickling method [1-3] and; (b) sandblasting [4-6]. In the former approach, sand is allowed to trickle over the surface of the glass from a controlled height to simulate erosion, while in the latter method the sand is propelled by compressed air towards the surface of the glass. The flaw morphology during sandblasting resembles flaws induced by sharp indenters and may induce radial and lateral cracks [6]. The erosive resistance of the glass was found to be a function of the particle size, the impact velocity, duration of abrasion and impact angle [1-7].

Besides surface erosion, glass components are also exposed to the risk of flaws during installation, cleaning and in-use conditions of the building. This type of flaws occurs when objects of higher hardness than glass are forced onto the glass and/or dragged along its surface. Scratch resistance is usually assessed with indenters and commercially available custom-made scratching devices that can accommodate geometrically different indenters [8-10].

Three regimes have been identified during the evaluation of the scratch resistance [11]:

- micro-ductile regime: irreversible deformation is caused by the indenter. Lateral cracks may be created beneath the surface however, there is absence of radial or median cracks;
- micro-cracking regime: significant damage is caused by the indenter; the lateral cracks extend and intersect with the surface while radial cracks are also formed and;
- micro-abrasive regime: debris is formed along the length of the scratch induced by the indenter.

The scratch resistance of glass is influenced by the tip of the indenter, the type and chemical compositions (silica content) of the glass and the ambient relative humidity [9, 10 & 11]. Glasses with higher silica concentration require higher loads for the formation of radial and lateral cracks. The formation of the flaw is also dependent on the indenter tip. Different tip angles can result in different scratch regimes. Indenters with 90° or 120° tips produce scratches belonging to the micro-cracking regime, resembling the ones produced during the cleaning process [9].

Despite the available research on the weathering mechanisms of glass, only one standard (DIN 52348 [12]) proposes an artificial ageing method for glass. In this standard, falling abrasive is allowed to trickle over the surface of the glass inducing the artificial damage. The effect on the glass surface is then evaluated by measuring the amount of light that is scattered during a light transmittance test, but the mechanical strength of the glass is not evaluated. Additionally, no actual correlation is available between naturally induced damage that accumulates on the glass surface during its service life and damage induced by this artificial ageing method. This raises questions on the ability of this method to produce realistic damage. This paper aims to evaluate this artificial ageing method of glass and also try to identify other artificial ageing methods. The methods investigated involve: (a) an adaptation of the DIN52348 [12] sand trickling method; (b) the use of a custom-made scratching device. For the evaluation of these methods, naturally aged annealed glass is used as a reference.

2. Evaluation of naturally aged specimens

The strength and roughness parameters of naturally aged, soda-lime-silica glass specimens were undertaken on 3 mm thick glass obtained from a façade in Norfolk, UK which was in service for 20 years. The specimens were cut to size (150x150 mm) using a diamond cutter. The glass was cleaned with common glass cleaning agents and warm water in order to remove the organic and inorganic residue that accumulated on the external surface of the glass during its service life. It was not possible to distinguish the tin and the air side under a UV light as a result of the extensive weathering of the surface of the glass. The residual stress profile of the specimens was determined with a scattered light polariscope (SCALP 05, GlasStress Ltd.) at the centre of each specimen. A surface compression of 7.5±0.5MPa was recorded for the naturally aged specimens. The external surface was distinguished from the internal under naked eye observation.

2.1. Surface roughness characterization

The surface roughness was determined individually for all the naturally aged specimens using a Form Talysurf PGI 820 surface profilometer (Taylor and Hobson Ltd.). The profilometer uses a 2 μm radius stylus to obtain the profile of the surface along the evaluation length (Fig. 1). Six evaluation lengths (each of 50 mm) were obtained in total along the *x* and the *y* direction on the surface of each specimen. These six lengths were spaced 15 mm apart to give a representative value of the area that would subsequently be tested destructively (§2.2).

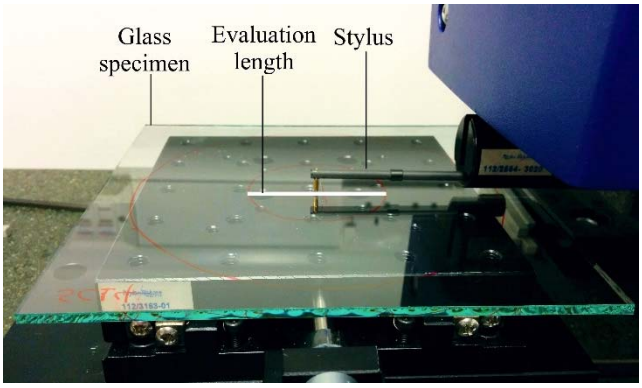

Fig. 1: Surface roughness characterisation.

Only two of the roughness parameters that were generated by the surface profilometer will be used in this paper [13]:

- R_a: the average roughness described by:

$$R_a = \frac{\sum_{i=1}^{n} |z_i|}{n} \quad (1)$$

where n: the number of measured points within the evaluation length and z: the vertical distance of each measured point from the mean line of the profile.

- R_v: the maximum valley height i.e. the vertical distance difference between the lowest point of the measured profile from the mean line described by:

$$R_v = \left|\min\left(z_i\right)\right| \tag{2}$$

2.2. Coaxial double ring test

The naturally aged glass specimens were then tested to failure in a coaxial double ring setup (Fig. 2a). A self-adhesive transparent film was applied on the compressive surface of the specimen prior to the testing to allow fractographic analysis and determination of the origin of failure. This is crucial as only specimens that fail within or underneath the loading ring will be considered for further strength analysis.

The dimensions of the loading and the reaction rings (D_L=51 mm and D_S=127 mm) comply with the ASTM C1499-03 standard [14]. A hinge was incorporated above the loading ring to allow self-alignment of the ring on the glass surface during the test. Testing was performed in quasi-inert conditions in order to avoid the influence of sub-critical crack growth caused by load duration and humidity. In the current set-up, quasi-inert conditions were achieved by inducing fracture rapidly (within 3-5 sec). The displacement rate for this range of time-to-failure was determined from a finite element analysis performed in Abaqus SIMULIA version 6.12. This corresponds to a stress rate of approximately 10 MPa/sec and a displacement rate of approximately 13.6 mm/min. A strain gauge was used at the centre of the loading ring on the tensile surface of one specimen. The experimental strain data were then used to validate the FEA model which was to be further employed to predict the failure stress for each of the specimens that was tested experimentally based on their failure load.

(a)

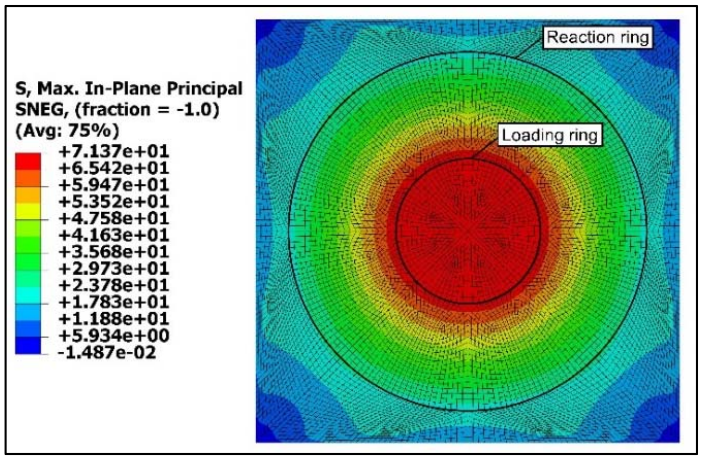

(b)

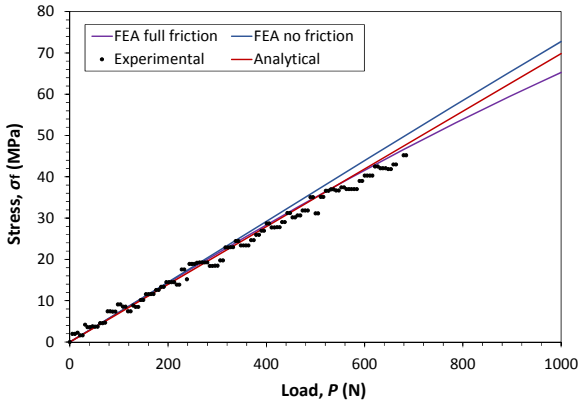

(c)

Fig. 2 (a) Coaxial double ring set-up; (b) FEA stress contours of coaxial double ring test (P=1000 N) and; (c) Maximum tensile stress, σ_f vs. load, P, results.

The FEA models consisted of 10,064 quadratic quadrilateral shell elements (S8R). A non-linear general elastic analysis was chosen for the model while the load was divided in 20 load steps of 100 N. Two separate models were

created in order to simulate the two extreme cases of friction conditions between the interface of the glass and the loading or the reaction ring (full friction contact and frictionless contact). The two FEA models produce the expected equibiaxial stress field and showed an almost uniform stress field within the loading ring (Fig. 2b). The load vs. stress relationship of the full friction model provided a better fit to the one derived from the experimental data when compared to the analytical computations based on the ASTM C1499-03 standard for the equibiaxial flexural strength of glass [15] and the no friction model (Fig. 2c).

The full friction model was therefore used in subsequent parts of this study to determine the failure stress of each specimen by accounting for the measured thickness and failure load. Six models of different thickness were simulated in Abaqus in order to accommodate differences in the thickness of the naturally aged specimens that fluctuated between 2.75 and 3.00 mm. The failure stress for the measured thickness of each specimen was found based on linear interpolation between the results of these 6 models.

3. As-received annealed glass and artificially aged annealed glass

Artificial ageing was performed on as-received soda-lime-silica annealed glass specimens that were supplied in the required 150 x 150 x 3 mm size. The residual stress profile in this case was found to be 2.5 ± 1 MPa. Table 1 summarizes the different sets of specimens that were tested experimentally.

The first set comprises the control set of as-received annealed glass (AR). These specimens were tested in their as-received condition using the same sequence of non-destructive and destructive tests that were previously described for the naturally aged glass to obtain their original roughness and strength characteristics.

The remaining specimens were artificially aged. Two artificial ageing methods of as-received annealed glass were used for the purpose of this study as follows: a) the induction of a random flaw population on the surface of the specimen created by the impact of falling abrasive and; b) the induction of a single flaw on the glass surface with a custom-made scratching device. The two artificial ageing methods are described in more detail in §3.1 and §3.2. After the artificial ageing the specimens were evaluated with the same sequence of testing (i.e. surface roughness characterization followed by coaxial double ring tests) that were performed on the naturally aged glass series and described in §2.

Table 1: Series overview.

Series	Description	No. of sets	No of specimens/set	Dimensions [mm]	Ageing method
AR	As received	1	10	150 x 150 x 3	No ageing
NA	Naturally aged	1	15	150 x 150 x 3	Natural ageing
SA_{a-c}	Sand abraded	3	15	150 x 150 x 3	Sand trickling
SC_{a-b}	Scratched	2	15	150 x 150 x 3	Scratching device

3.1. Artificial ageing with the sand trickling method

The sand trickling method (also known as the dropped grit method) involves the formation of a random population of flaws by dropping a controlled mass of abrasive material over the surface of the glass specimen from a specific height. The methods used in this study are adapted from the methods described in the German DIN 52348 standard "Testing of glass and plastic wear" [12].

The sand trickling rig (Fig. 3) comprises: a) a sand container where the abrasive material is stored; b) a steel valve which is bolted to the lower part of the sand container to allow control of the sand flow with the use of a manually-operated handle; c) a circular tube with an inner diameter of 82 mm used to guide the falling abrasive and prevent it from dispersing disorderly and; d) a specimen holder / base (stationary or rotating) where the specimen is clamped inclined at a 45^{o} angle to the ground with the tin side exposed to the falling abrasive. For the rotating version of the base, a motor was attached to the base to incorporate rotation of the specimen. The rotation speed is set to 250±5 rpm based on the recommendations of DIN 52348 and is validated with a stroboscope.

The ageing process is completed when the full mass of the abrasive in the container has trickled onto the tin side of the glass. Three sets of specimens (SA series) were tested with this artificial ageing method. Three kilograms of silica sand were used for the ageing of all the specimens according to the DIN 52348 while the grain size ranged between 0.50 to 1.00 mm. The height of the guide tube ranged between 1.1 m and 3.0 m. Table 2 summarizes the testing details for each set.

Table 2: Sand abraded (SA) series details.

Series	No of specimens/set	Drop height (m)	Mass of falling abrasive (kg)	Grain size range (mm)	Specimen holder
SA_a	15	3.125	3.00	0.50-1.00	stationary
SA_b	15	3.125	3.00	0.50-0.70	rotating
SA_c	15	1.225	3.00	0.50-0.70	rotating

3.2. Artificial ageing with scratching device

Two sets of specimens (SC series) were scratched with the use of a custom-made scratching device similar to the ones used in [8 & 15]. The scratching device (Fig. 4a) features a 90° tungsten carbide tip which is attached to the stem of the device incorporating dampers to allow the adjustment of the tip on the glass surface. The specimen is clamped along two edges with two steel plates while the device is dragged manually at a speed of approximately 4 mm/sec on the tin side of the glass specimen inducing a single flaw on its surface. PTFE tape was used to cover the supporting legs of the scratching device to reduce friction when in contact with the glass and avoid the induction of additional flaws. The length of the flaw is controlled mechanically with the steel clamping plates and is kept constant for both sets of specimens (20 mm). A mass of 1.0 kg was placed on the platform, resulting in a total weight of 1.6 kg when the self-weight of the platen and the stem of the device are also taken into account. The difference between the two sets (SC_a and SC_b) is the sharpness of the indenter. A blunt 90° tip angle indenter was used for SC_a while a sharp 90° tip angle indenter was used for SC_b. (Fig. 4b).

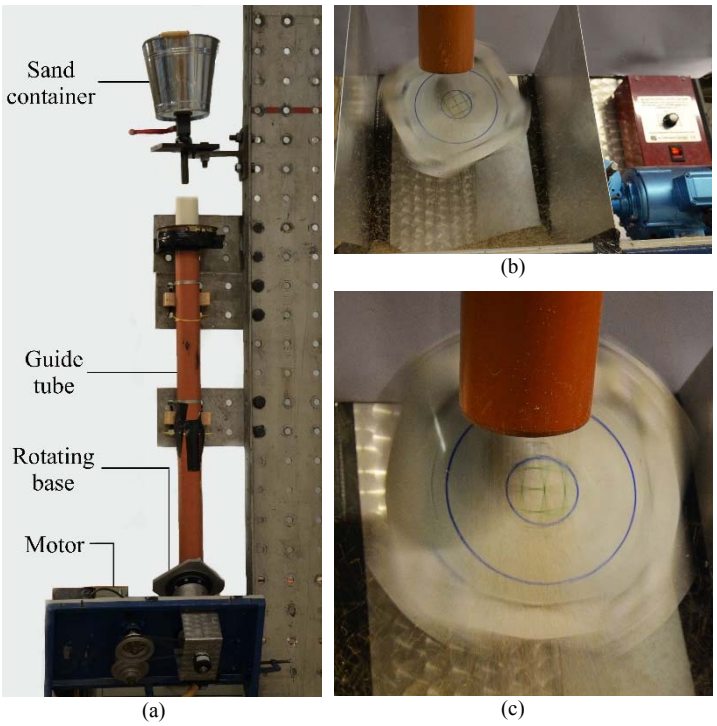

Fig. 3: (a) Sand trickling rig; (b) rotating base with motor and; (c) sand abrasion.

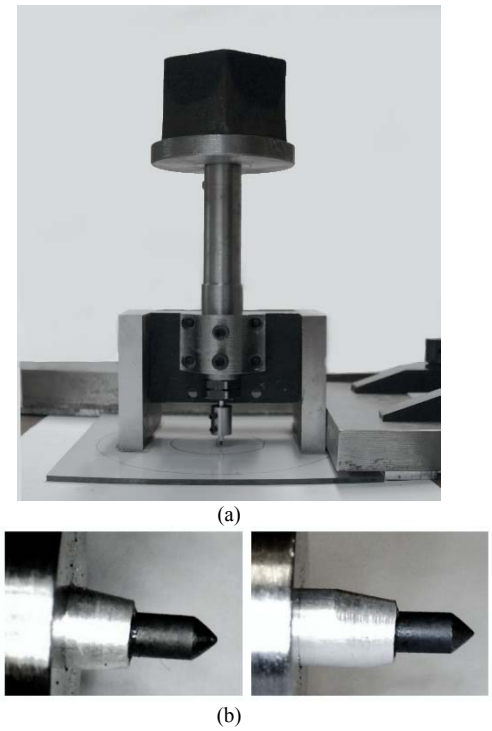

Fig. 4 (a) Scratching device and; (b): Blunt (left) and sharp (right) 90° indenter tip.

4. Results and discussion

4.1. Microscopy observation

A Leica optical microscope was used to obtain qualitative images of the surface of all the tested series (Fig. 5a-f). The internal surface of the naturally aged glass that was protected from weathering action resembles the surface of the new as-received annealed glass (Fig. 5 a & b). As expected, more extensive damage is noticed on the external surface of the naturally aged specimens consisting mostly of pits and some scratches. (Fig. 5c). Pits were only noticed on the surface of the SA series at the points of impact of the sand grains (Fig. 5d). The damage was found to be more extensive when the grain size of the sand and the drop height were increased. Finally, the sharpness of the indenter changed the cracking regime of the damage. A micro-ductile regime was observed for the blunt indenter with absence of radial or

median cracks (Fig. 5e) whereas a micro-cracking regime was observed for sharp indenters with radial crack and chip formation (Fig. 5f).

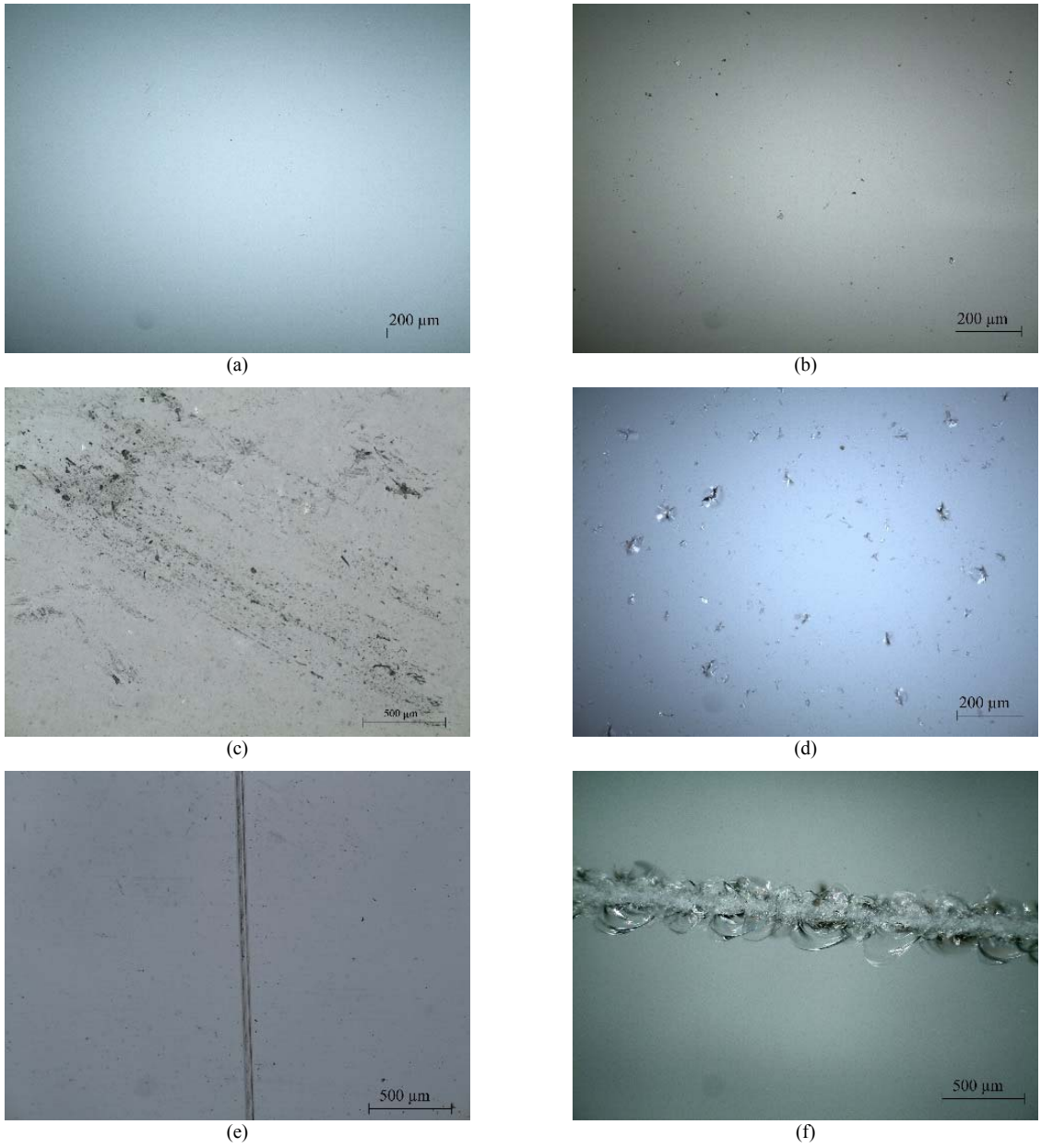

Fig. 5: Optical microscopy of the: (a) as-received annealed glass - tin side (AR); (b) internal "protected" surface of the naturally aged glass (NA); (c) outer "exposed" surface of the naturally aged glass (NA); (d) sand abraded glass (SA_b); (e) the scratched glass with a blunt indenter (SC_a) and; (f) the scratched glass with a sharp indenter (SC_b).

4.2. Surface roughness data

Table 3 summarizes the roughness parameters for each set of specimens. These were reported to be the lowest for the AR series. The NA series showed an average-roughness increase of 680% while the increase in maximum valley height is 349%. However, none of the tested methods managed to simulate the roughness of the NA series (Fig. 6 a & b). The closest match was provided by the sand abraded series SA_c which corresponds to a drop height of 1.225 m while significantly larger values were observed for the rest of the SA series ($SA_{b\text{-}c}$, 3.125 m drop height).

The SC series displayed a substantial increase in the maximum valley height when a sharp indenter is used (SC_b) which was almost 7 times larger than the one reported for the NA series. The opposite applies for the blunt indenter (SC_a) as the increase in the maximum valley height was almost 9 times lower than the one reported for the NA series. Furthermore, average surface roughness was found to be a poor evaluation measure of the SC series as a single flaw is only induced on the surface of glass. This is also displayed in Table 3 as the R_a results are lower than those of the NA or SA series.

Table 3: Roughness parameters results.

Series	$R_{a,av}$	% roughness increase $R_{a,av}$	$R_{v,max}$	% roughness increase $R_{v,max}$
NA	0.0156	680	0.0893	349
AR	0.002	0	0.0199	0
SA_a	0.0517	2485	2.064	10272
SA_b	0.0276	1280	0.8327	4084
SA_c	0.0093	375	0.3169	1492
SC_a	0.0062	210	0.0279	40
SC_b	0.0095	375	0.64	3116

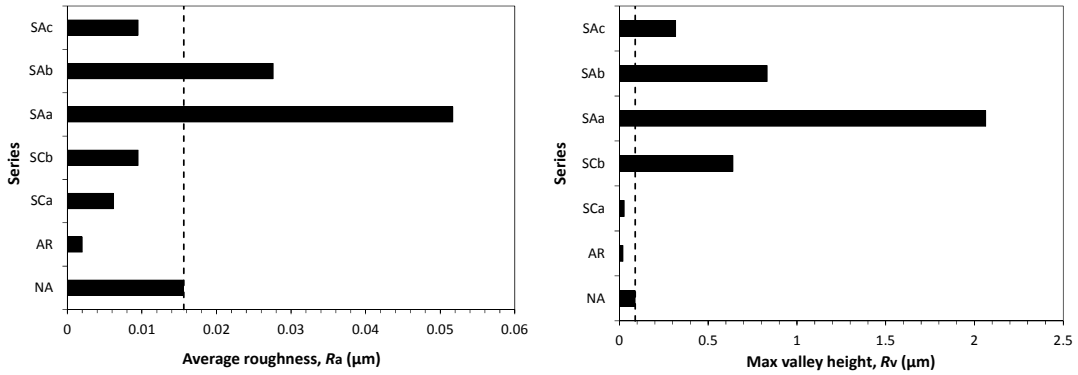

Fig. 6: Comparative roughness results for all tested series: (a) average roughness and; (b) maximum valley height.

4.3. Statistical analysis of strength data

As expected the coaxial double ring tests produced a range of times to failure, t_f. Therefore, the failure stress that was exerted on each specimen had to be converted to a constant uniform stress corresponding to a reference time to failure using Eq. 3 [16] (in this case the reference time of t_{eq}=60 sec was chosen) in order to allow comparison and statistical analysis of the strength results:

$$\int_0^{t_f}\left(\frac{\sigma_f \cdot t}{t_f}\right)^n dt = \int_0^{t_{eq}} \sigma_{f,eq}^n dt \Rightarrow \sigma_{f,eq} = \sigma_f \cdot \left[\frac{t_f}{t_{eq}\cdot(n+1)}\right]^{1/n} \tag{3}$$

where $\sigma_{f,eq}$ is the equivalent stress under t_{eq}=60 sec of uniform stress loading, σ_f is the unmodified failure stress obtained experimentally and n is the exponential crack velocity parameter (n=16 for normal conditions).

A two-parameter Weibull distribution was then fitted to these equivalent strengths:

$$P_f(\sigma_{f,60\sec}) = 1 - \exp\left\{\left(-\frac{\sigma_{f,60\sec}}{\theta}\right)^{\beta}\right\} \tag{4}$$

where P_f: the cumulative probability of failure, θ: the scale parameter and β: the shape parameter.

The specimens were ranked in ascending order and assigned a corresponding cumulative probability of failure. The estimator used in this paper was chosen according to the recommendations of EN 12603:2002 [17] and is described by:

$$G(x_i) = \frac{i-3}{n+0.4} \tag{5}$$

where i is the ith value of the ordered stress sample.

Table 4: Weibull parameters and characteristic fractile values overview.

Series	Shape factor β	Scale factor θ	Goodness of fit p_{AD}	Fractile strength $\sigma_{f,0.001}$	% $\sigma_{f,0.001}$ reduction	Fractile strength $\sigma_{f,0.5}$	% $\sigma_{f,0.5}$ reduction
NA	3.683	43.230	0.059	6.627	66	39.135	65
AR	9.038	115.008	0.458	53.559	0	110.438	0
SA_a	16.126	31.880	0.616	20.773	46	31.164	72
SA_b	17.570	35.647	0.686	24.060	42	34.911	68
SA_c	34.777	48.422	0.773	39.699	19	47.914	57
SC_a	2.087	49.371	0.358	1.804	73	41.419	62
SC_b	9.878	24.517	0.133	12.184	58	23.624	79

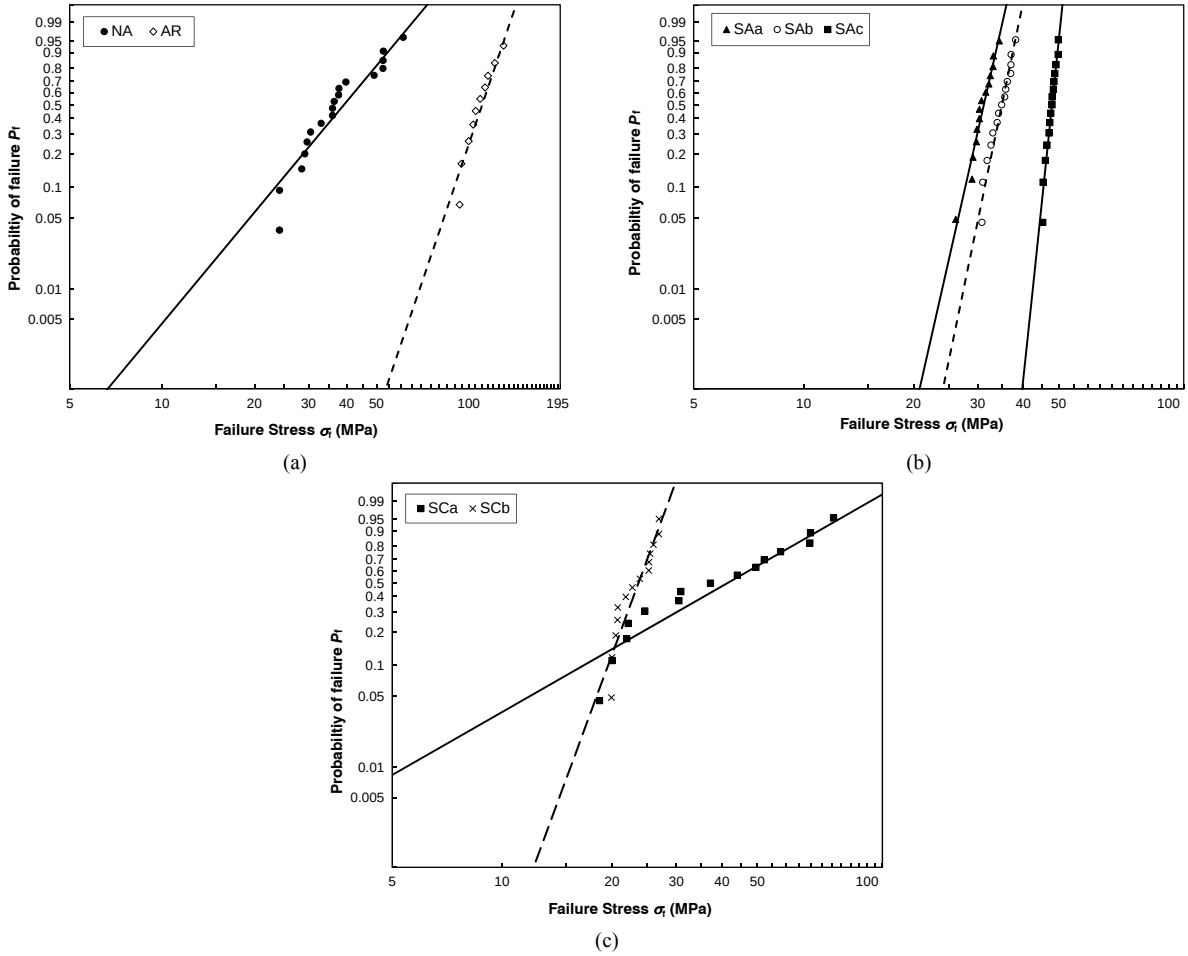

Fig. 7 Webull plots for: (a) Naturally aged (NA) series and as-received series (AR); (b) Sand abraded series (SA) and; (c) Scrathed series (SC).

The shape (β) and the scale (θ) parameters of the Weibull distribution were then computed according to the approach described in EN 12603:2002 [17] in order to produce a linear logarithmic distribution with a gradient of β (Fig. 7a-c). The Anderson-Darling p_{AD}, with a 5% rejection error threshold was used to assess goodness-of-fit. Low, but still acceptable, values of goodness of fit, p_{AD}, were only reported for the NA and the SC_b series (Table 4). This can be justified for the former as the damage induced in the NA glass panels during their service life is random across the surface and not homogeneous. The same applies for the SC_b series as the sharp indenter did not create a uniform and homogeneous scratch along the surface of the SC_b specimens but induced many uncontrolled lateral and median flaws leading to chip formation. Furthermore, the shape factor of the NA series was significantly lower than the rest of the

artificially aged series (except SC_a). This shallow gradient of the distribution represents a larger variation in strength, and can be once more attributed to the non-uniform damage on the surface of the NA specimens.

Table 4 summarizes the representative values of the Weibull distribution for each of the tested series as well as the noteworthy strength results corresponding to 1‰ and 50% fractile values of the Weibull distributions for all the tested series. These probabilities of failure are used to describe the design strength and the mean strength of glass respectively. The percentage of strength reduction was then computed for the naturally and the artificially aged series using as a reference the as-received AR series (Table 4).

For the naturally aged series, a 65% reduction in the mean strength with respect to the new as-received AR series was noted, whereas for the artificially aged series, the strength reduction ranged between 57-79%. In particular, the sand abraded series (SA) displayed a 57-72% strength reduction, the highest corresponding to SA_a and the lowest to SA_c. This can be explained as follows for: (a) the SA_a series, as the sand grain size was larger than the $SA_{b\text{-}c}$ series and the induced damage was concentrated in a smaller area when compared to $SA_{b\text{-}c}$ where the specimen was fixed on a rotating base which was resulting in uniformly spread damage over the surface of the specimen and; (b) the SA_c series, as the drop height was the lowest that was tested minimizing the damage induced on the surface. A more significant mean strength reduction (79%) was noted for the SC series scratched with the sharp indenter (SC_b series) causing a higher strength degradation than the blunt indenter (SC_a series, 62%). However, the opposite applies as the probability of failure decreases. This is due to the shape factor of the Weibull distribution being fairly low (2.097) for the SC_a series which causes a larger variation in strength. Overall, the best fit for mean strength was provided by the SA_b and the SC_a series.

However, even though adequate agreement was found for the mean strength results, this was not the case when lower fractile values (1 ‰ probability of failure) are considered. All of the artificially aged series, except SC_a which provided a relatively good fit, resulted in higher strength at the lower probabilities of failure when compared to the NA series. This can be attributed to the shallow gradient (low value of shape factor β) of the NA distribution and consequently the large variation in strength. Therefore, further investigation is needed in order to achieve lower shape factors (β) for the artificially aged series.

4.4. Artificially aged series (S series) evaluation

Table 5 contains a ranking list for all the series that were tested experimentally based on their average surface roughness and mean strength results. The closest match to the NA series for both strength and average surface roughness is provided by SA_b. This ranking system also shows that average roughness R_a and the maximum valley height R_v is inversely related to mean strength for the SA series and the SC series respectively.

Table 5: Evaluation of the artificially aged series for roughness and strength (highest to lowest values)

Parameter	**Ranking of SA series (highest to lowest values – left to right)**						
Average Surface Roughness R_a	SA_a	SA_b	**NA**	SC_b	SA_c	SC_a	AR
Mean Strength $\sigma_{f,0.5}$	AR	SA_c	SC_a	**NA**	SA_b	SA_a	SC_b
Max valley height R_v	SA_a	SA_b	SC_b	SA_c	**NA**	SC_a	AR

5. Conclusions

Two artificial ageing methods have been investigated in this paper involving the induction of a flaw population on the surface of the specimen caused by falling abrasive (sand trickling method - SA series) and induction of a single flaw on the surface of the specimen with a scratching device (SC series). The naturally aged glass (NA) showed a 65% reduction in mean strength with respect to the as-received new glass (AR). This reduction ranged between 62-79% for the artificially aged series. The average surface roughness (R_a) was found to be a satisfactory comparison measure of the mean strength of glass when damage is induced by sand trickling; wherein the average surface roughness is an inverse indicator of glass strength. The same applies for maximum valley height (R_v) when only a single flaw is induced on the glass surface (SC series).

Two measures can be used to determine correlation between the naturally aged and the various sand abraded and scratched series, namely: means strength and surface roughness. It was found that the best correlation for mean strength was achieved by the SA_b series with the highest drop height (3.115m) and the narrowest grain size range (0.50-0.70 mm) during sand abrasion and the SC_a series that were scratched with a blunt indenter. Whereas the best correlation for average surface roughness was provided by the SA_c series with the lowest drop height (1.225m) and the narrowest grain size range during sand abrasion. Overall, the SA_b series is deemed to be the best performing among the artificially aged series of glass when both strength and surface roughness are considered.

Future work includes investigation of combinations of the artificial ageing methods that were considered in this paper and also identification of potential ways of randomizing the experimental strength data produced by the artificial ageing methods in order to decrease the shape parameter β of the Weibull distribution and accurately simulate the behaviour of naturally aged glass.

Acknowledgements

The authors gratefully acknowledge Shiqi Li's contribution during part of the experimental testing and also financial support from Eckersley O'Callaghan, the Research Fund for Coal and Steel of the European Community and the Engineering and Physical Sciences Research Council UK (EPSRC).

6. References

[1] Völker C, Philipp D, Masche M, Kaltenbach T. Development of a test method for the investigation of the abrasive effect of sand particles on components of solar energy systems; Proc 29th Eu PV Solar Energy Conf; 2014; Netherlands.

[2] Roumili F, Benbahouche S, Sangleboeuf J C. Mechanical strength of soda-lime glass sandblasted by gravitation. Friction; 2015; 3 (1); 65-71.

[3] Protopopescu N. Sand Trickling Abrasion Testing of Float Glass. Some methodological and experimental considerations. Proc Glass Processing Days; Finland; 2001; 261-65.

[4] Bousbaa C, Madjoubi A, Hamidouche M, Bouaouadja N. Effect of annealing and chemical strengthening on soda lime glass erosion wear by sand blasting. J Eu Ceram Soc; 2003; 23; 331-43.

[5] Bouzid S, Bouaouadja N. Effect of impact angle on glass surfaces eroded by sand blasting. J Eu Ceram Soc; 2000; 20; 481-8.

[6] Adjouadi N, Laouar N, Bousbaa C, Bouaouadja N, Fantozzi G. Study of light scattering on a soda lime glass eroded by sandblasting. J Eu Ceram Soc; 2007; 27; 3221-9.

[7] Sparks A.J, Hutchings I.M. Transitions in the erosive wear behaviour of a glass ceramic. Wear; 1991; 149 (1-2); 99-110.

[8] Overend M, Louter C. The effectiveness of resin-based repairs on the inert strength recovery of glass. Construction and Building Materials; 2015; 52; 165-174.

[9] Schneider J, Schula S, Weinhold W P. Characterisation of the scratch resistance of annealed and tempered architectural glass. Thin Solid Films; 2012; 520, 4190-8.

[10] Schneider J, Schula S. Characterisation of the scratch resistance of annealed and tempered architectural glass. Proc Glass Performance Days; 2011; Finland; 139-43.

[11] Le Houérou V, Sangleboeuf J C, Dériano S, Rouxel T, Duisit G. Surface damage of sodalime- silica glasses: indentation scratch behaviour. J Non-Cryst Solids; 2003; 316; 54-63.

[12] DIN 52348, 1985. Standard for Testing of Glass and Plastics; Abrasion Test; Sand Trickling Method, Deutsches Institut Fur Normung; 1985; www.din.de.

[13] H. Dagnall. Exploring surface texture. Rank Taylor Hobson Ltd; England; 2009.

[14] ASTM Standard C 1499-03, 2001. Standard Test Method for Monotonic Equibiaxial Flexural Strength of Advanced Ceramics at Ambient Temperature. ASTM International; West Conshohocken; PA; 2010; DOI: 10.1520/D0968-05R10; www.astm.org.

[15] Haldimann M. Fracture strength of structural glass elements – analytical and numerical modelling, testing and design. Thèse EPFL No 3671, Ecole polytechnique fédérale de Lausanne (EPFL), 2006.

[16] Haldimann M, Luible A, Overend M. Structural Use of Glass. International Association for Bridge and Structural Engineering IABSE; 2008.

[17] CEN (European Committee for Standardization). Glass in building – Procedures for goodness of fit and confidence intervals for Weibull distributed glass strength data; EN 12603; 2002; 2002.